A Deep Learning Based Effective Model for Brain Tumor Segmentation and Classification Using MRI Images

Gayathri T. [1] and Sundeep Kumar K. [2,*]

[1] Department of Information Science and Engineering, MVJ College of Engineering, Bengaluru, India
[2] Department of Computer Science and Engineering, Geethanjali Institute of Science and Technology, Bengaluru, India;
Email: principalgist@gist.edu.in (S.K.K.)
*Correspondence: gayal28@gmail.com (G.T.)

Abstract—**A brain tumor is formed by an excessive rise of abnormal cells in brain tissue. Early identification of brain tumors is essential to ensure patient safety. Magnetic Resonance Imaging (MRI) scan is used to diagnose brain tumors. Unfortunately, because of the varying form of tumors and their location in the brain, physicians are unable to provide good tumor segmentation in MRI images. Accurate brain tumor segmentation is required to identify the tumor and offer the appropriate therapy to an individual. In this research, a novel hybrid deep learning technique termed Convolutional Neural Network and ResNeXt (CNN-ResNeXt) is introduced to segregate and classify the tumor automatically. Firstly, the MRI image is collected from the standard datasets known as BRATS 2015, BRATS 2017 and BRATS 2019. Then the collected data is smoothed and enhanced by batch normalization technique and the features are extracted from the smoothened image based on tumor shape position, shape and surface features using AlexNet model. Next, using an Adaptive Whale Optimization (AWO) approach, the optimal features are selected for effective segmentation. Consequently, the image segmentation process is done using CNN–ResNeXt depending on the selected features. Finally, the segmented image is used for the classification which is also done by employing CNN-ResNeXt. Whereas compared to the other existing models, the proposed CNN–ResNeXt model achieved a greater accuracy of 98% for the tumor core class. This demonstrates that the proposed methodology segregates and classifies brain tumors effectively.**

Keywords—**Adaptive Whale Optimization (AWO), AlexNet, brain tumor, Convolutional Neural Network (CNN), Magnetic Resonance Imaging (MRI), and ResNeXt**

I. INTRODUCTION

The brain is a major organ consisting of nerve cells with supporting tissues such as glial cells as well as meninges. Damage to these specific brain subparts is irreversible and can lead to severe conditions, including life-threatening brain tumors [1]. Brain tumors are formed by abnormal cells that develop in the human brain [2]. The present occurrence of malignant tumors is excessive, which has a significant impact on persons as well as the community [3–6]. The most essential clinical image method for detecting brain cancers is Magnetic Resonance Imaging (MRI). MRI seems to be a secure as well as non-invasive diagnosis technology that delivers more sufficient data on brain tissues than computed tomography scans [7–9]. The precise segmentation of brain tumors from clinical images are required to give a statistical and understandable guideline for medical diagnosis and therapy of disorders [10]. As a result, precise segmentation of brain tumors is an important phase in brain tumor diagnosis and therapy [11]. However, the precise segmentation of brain tumors is still considered a highly difficult process, because of various reasons such as changes in tumor form, size, and location, hazy borders [12], and so on. In recent decades, some brain tumor segmentation approaches have been presented. Traditional techniques based on handmade features as well as Machine Learning (ML) models: Support Vector Machines (SVMs) and Random Forests (RFs) typically perform poorly [13]. Deep Learning (DL) approaches for the segmentation of medical images have attracted a lot of interest in current decades, due to many studies with remarkable results for detecting and estimating target structures in images [14]. The level of user engagement with the system and the ease of use of segmentation methods often influence their adoption in medical applications. Manual brain tumor segmentation is a time-consuming method that requires researchers to physically identify the Region of Interest (ROI) on MRI segments utilizing advanced graphical user interface tools. Manual segmentation requires a lot of time [15] and is vulnerable to user errors, which include inter and intra-variations. An autonomous approach for brain tumor segmentation might reduce the limitations of human errors while being immune to external influences which include disturbances as well as the physician's mental state. Under the related works area, current studies have developed several efficient automatic systems. As a result, a practitioner constructing an autonomous segmentation system really

shouldn't concentrate only on creating a model that learns and does the segmentation autonomously. More efforts must be put towards delivering enhancements such as, modifying the model's design to utilize lower assets and provide greater accessibility to users [16]. As a result, the current study offers a model based on deep Convolutional Neural Network (CNN) and ResNeXt for segmentation and effective classification. The main contributions included in this research are stated as follows:

- A deep learning-based CNN with ResNeXt is proposed for effective brain tumor segmentation and classification using MRI images.
- The MRI images are collected from the BraTs 2015, BraTs 2017, and BraTs 2019 datasets where both are publically available standard datasets.
- In the preprocessing phase, the batch normalization technique is used whereas the feature extraction phase is done using the AlexNet model which extracts the features from the preprocessed MRI images.
- Later, the feature selection process is performed using the AWO which selects the optimal features for effective segmentation and classification.

The organization of the research is as follows: Section II describes the related works of the methods used for the detection and classification of brain tumors. Section III offers a detailed explanation of the proposed methodology. In Section IV, the simulation results are described. Finally, the overall conclusion is provided in Section V.

II. RELATED WORKS

Khairandish *et al.* [17] presented a hybrid CNN-SVM model for the detection as well as classification of brain tumors. The BraTs 2015 dataset is utilized in this study which is publically available. The key preprocessing procedures were conducted to normalize the input images, then relevant features were extracted from the preprocessed image through the Maximally Stable Extremal Regions (MSER) approach, and then for segmentation threshold-based segmentation algorithm was used. To categorize brain MRI images, the labeled segmented features are fed into hybrid CNN & SVM methods. The suggested hybrid model demonstrates that merging the benefits of CNN and SVM can result in superior models with classification accuracy of 98.4%. However, when additional evaluation criteria such as PPV and FPV were considered, the classification performance for these parameters was similar for CNN, SVM, and hybrid CNN-SVM.

Ilyas *et al.* [18] established a Hybrid Weights Alignment with Multi-Dilated Attention Network (Hybrid-DANet) to perform segmentation automatically. The performance of the Hybrid-DANet is validated on two well-known datasets (BraTS 2017, 2018). Next, a Multi-Channel Multi-Scale (MCS) component was added to the basic component whereas the Residual Module (RM) was utilized to decrease the saturated accuracy caused by the vanishing gradient issue. Hence, the RM, as well as MCS, are beneficial for obtaining the deep, intrinsic, channel-wise feature while avoiding depth as well as height extension. On the BraTS 2018 dataset, HWADA achieved comparable Dice Similarity Coefficient (DSC) results of 0.892, 0.764, 0.680 for the Whole Tumor (WT), Tumor Core (TC) and Enhanced Tumor (ET), respectively, because the basic to deeper characteristics were extracted. However, the suggested model was only evaluated for an encoder component in this study.

Almajmaie *et al.* [19] created a hybrid deep learning architecture for segmenting brain tissue that combines SegNet with U-Net algorithms. The proposed SegNet-UNet technique was assessed using the BRATS 2017 and BRATS 2018 datatsets. In this case, a skip connection of the relevant U-Net network was thoroughly investigated. Whenever pooling indices flow via de-convolution layers, the model achieved quicker convergence. After that, by merging more level set layers inside this design, counters of brain tissue borders are retrieved. The suggested SegNet-UNet model achieved a better DSC of 0.82, 0.73 and 0.68 for WT, CT, and ET, respectively. The findings show that by combining level sets with repetitive FCN architectures, the suggested DRLs provide a better solution in terms of resilience over anomalies, speed, and consistency in segmenting core tumors. Furthermore, DRLs significantly enhance the pace of segmenting brain tumors, which makes it an effective method.

Lamia and Barzegar [20] established a semi-supervised multi-labeling system named Weighted Label Fusion learning Framework (WLFS) for automated glioma segmentation. The proposed technique was assessed using the datatsets such as BRATS 2015, BRATS 2017 and BRATS 2019. The system was divided into three sections: image preparation, graph creation, as well as segmentation. By estimating the transmitted data, the labels were extended between the atlas as well as target images. The suggested WLFS achieved a better segmentation accuracy of 90.1%, 88.7% and 89% for WT, TC, and ET, respectively. Because data propagates repeatedly from vertices with great trust, to vertices exhibiting little trust, segmentation accuracy may be steadily increased in target images that are less closely related to atlas images. Due to the suggested approach's time evaluation, the running time was strongly dependent on the total amount and size of the samples.

Shehab *et al.* [21] presented a ResNet-based automated system for brain tumor segmentation. To validate the efficacy of the suggested approach, simulation experiments were run using the dataset BRATS 2015. An "identity shortcut connection" in ResNet allowed the gradient to be back-propagated to previous layers. The shortcut connection in the ResNet model managed the vanishing gradient issue. It enabled the exhibited model to acquire an identity function, thus ensuring that the upper layer performed better than the bottom layer. Whereas, the suggested ResNet system achieved a greater segmentation accuracy of 84%, 90%, 86% for TC, ET, and WT, respectively. Furthermore, feature extraction of LGG brain tumors demanded a little alteration in model architecture to enhance segmentation results.

Brain tumor segmentation using K-means clustering and deep learning with synthetic data augmentation for classification has been demonstrated by Khan *et al.* [22]. In the experimentation, the proposed technique was assessed using the BraTS 2015 data. Here, the segmentation was done using k-means clustering and classification was done using a refined VGG19 (i.e., 19-layered Visual Geometric Group). Additionally, the synthetic data augmentation idea was introduced to expand the amount of data that could be used for classifier training to enhance accuracy. By performing this, the overall accuracy achieved by the suggested method was 94%. However, approaches for identifying and categorizing tumors in MR images are still required to be specific, efficient, and dependable.

A Multiscale 3D U-Net's design employs a number of U-net blocks to gather long-distance spatial data at various resolutions which was demonstrated by Peng *et al.* [23]. Then, to extract enough features, the feature maps were upsampled at various resolutions to understand and process the optimized features. On the BraTS 2015 testing set, 3D depth-wise separable convolution was utilized to lower the computational cost, temporal, and space complexity. The suggested multiscale 3D U-Net achieved a greater DSC of 0.85, 0.72, 0.61 for WT, TC, and ET, respectively. It was regrettable that many Low-Grade Gliomas (LGG) images lack an enhancing zone. Those issues reduce the model's ability to optimize by making the tumor core and augmenting region less dominant during the training phase.

Latif *et al.* [24] developed a novel brain tumor segmentation system using a Multi-Inception-UNET (MI-UNET) architecture. The system incorporates two key components to improve the accuracy of tumor segmentation. Firstly, a CNN was employed to classify slices as tumorous or non-tumorous, effectively reducing false positives within the system. Secondly, a novel architecture named MI-UNET is used to segment the tumorous slices. MI-UNET extends the baseline UNET architecture by integrating inception modules at each level. This integration enhanced the scalability and representation capability of the UNET model, led to more accurate tumor segmentation results. To train the MI-UNET model, a weighted dice loss function is utilized. Whereas, the suggested MI-UNET achieved the greater accuracy of 94% with data augmentation. Due to limitations in computational resources and time constraints, certain aspects, such as further observations, variations, and experimentations were left as potential future work.

III. PROPOSED METHODOLOGY

In this research, a batch normalization with a transfer learning-based classification is proposed for the effective classification of brain tumors. The BRATS 2015, BRATS 2017, and BRATS 2019 are considered for evaluating the proposed system. Initially, batch normalization is used for the images followed by the AlexNet model for extracting features from images. Next, an AWO algorithm is used for the effective selection of features. A novel approach named CNN with ResNeXt is proposed for segmentation and effective classification. The flowchart of the proposed model is illustrated in Fig. 1.
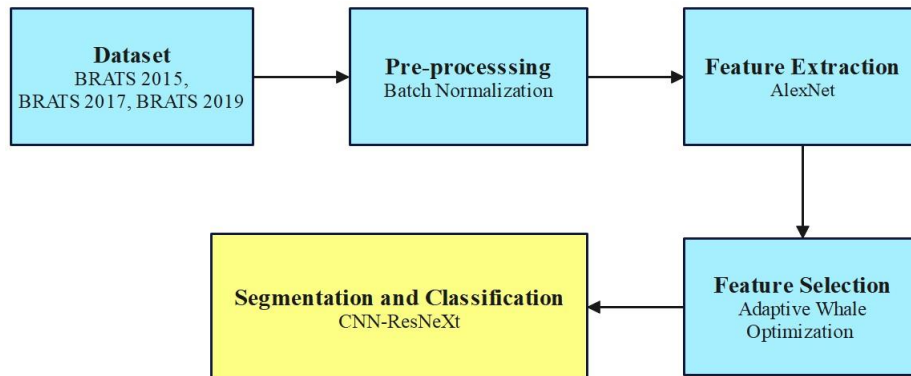

Figure 1. Flowchart of the proposed model.

A. Dataset

1) BRATS 2015

In this research, the standard publicly available dataset: BRATS 2015 (https://www.kaggle.com/datasets/xxc025/brats2015) is considered. The BRATS 2015 dataset is a widely used benchmark in the medical imaging community for evaluating brain tumor segmentation algorithms [25]. The overall amount of 2D FLAIR axial images of HGG, as well as LGG individuals in the 2015 dataset, was 220 as well as 54, respectively. T1, T1Gd, T2, as well as T2 FLAIR volumes, are the MRI scan modes/modalities used on every patient. Every image in this collection is 512×512 pixels in size, with pixel sizes of 49 mm × 49 mm.

2) BRATS 2017

The BRATS 2017 dataset (https://www.kaggle.com/datasets/abdullahalmunem/brats17) is an updated version of the BraTS dataset, with improvements and additional features. It consists of MRI scans from multiple institutions, focusing on brain tumor segmentation. Similar to BRATS 2015, the dataset includes T1-weighted, T1-weighted with contrast enhancement, T2-weighted, and FLAIR MRI sequences [26]. In BRATS 2017, the dataset has been expanded to include more cases, resulting in a larger and more diverse collection of brain tumor images.

Additionally, the ground truth manual segmentations have been enhanced to include more detailed tumor subregions. This enables more refined evaluation of segmentation algorithms and encourages the development of methods that can accurately identify different tumor components.

3) BRATS 2019

Similar to the above datasets, the BRATS 2019 dataset is an advanced version of the BRATS dataset. The BRATS 2019 dataset (https://www.kaggle.com/datasets/ aryanfelix/brats-2019-traintestvalid) offers several advancements over its predecessors. It includes a LGG and HGG of 76 and 259, respectively, allowing for more robust analysis and evaluation of brain tumor segmentation methods [27]. Additionally, BRATS 2019 introduces a survival prediction task, where participants are challenged to predict the overall survival time of patients based on their MRI scans. This expansion aims to foster the development of models capable of not only segmenting tumors but also predicting patient outcomes, potentially aiding in treatment planning and prognosis estimation.

B. Data Pre-processing

Batch normalization is the chosen pre-processing technique in this experiment, where the term batch refers to the set of input data and the process takes place in batches. Normalization is referred to as a tool that is used in converting numerical data to a common scale while preserving its shape. In other words, it is the process of transforming the data to have a 0 as the mean value and 1 as a standard deviation. The procedure of making Neural Networks (NN) faster and highly stable by adding more layers to the DNN is known as batch normalization. The standardization and normalization operations are performed by the new layer by considering the values of the previous layer. The mean and standard deviation of the hidden activation are calculated by taking batch input from layer h using Eqs. (1) and (2).

$$\mu = \frac{1}{m}\sum h_i \qquad (1)$$

$$\sigma = \left[\frac{1}{m}\sum(h_i - \mu)^2\right]^{\frac{1}{2}} \qquad (2)$$

where,

μ —mean,

σ —standard deviation,

m —number of neurons at layer h.

Using the values of Eqs. (1)–(2), the hidden activations are normalized. The mean value is subtracted from each input and then divide into the total value with the sum of the standard deviation and the smoothing term (ε). The smoothing term ensures the numerical stability inside the operation by preventing division by zero and it is calculated using Eq. (3).

$$h_{i(norm)} = \frac{(h_i - \mu)}{\sigma + \varepsilon} \qquad (3)$$

Then, the normalized images are sent to the further feature extraction process for extracting the features from these images.

C. Feature Extraction

AlexNet is a deep CNN architecture which plays a significant role in DL for computer vision tasks. Here, to extract the features from the preprocessed data, the AlexNet model is employed. It consists of 5 convolutional layers, 3 max-pooling layers, 2 normalization layers, 2 fully connected layers, and 1 softmax layer. The activation function was only the model's initial enhancement, which was then put to a NN for efficient evaluation. The AlexNet model contains 96 neurons, which trained for 100 epochs, and incorporates a dropout rate of 0.5. Conventional activation functions include the arctan function, $tan\,tan\,h$ function, as well as the logistic function. DL models encounter the disappearing gradient issue because of the presence of huge gradient values whenever input data is close to zero. The Rectified Linear Unit (ReLU) is used, and the activation function for the ReLU is stated in Eq. (4).

$$ReLU(x) = max\,(x, 0) \qquad (4)$$

If the input data is greater than zero, the ReLU gradient is updated to 1. The ReLU in deep networks has a higher convergence rate than the Tanh unit, which speeds up the training procedure. The feature map of a nearby pixel group is reduced in the pooling layer, and several approaches are utilized to create a value. In max pooling, each 2×2 block max value is created, as well as a 4×4 feature map is used to minimize feature dimension. Where, AlexNet's feature extraction process is fixed and not adaptive to the specific dataset. So, an Adaptive Whale Optimization (AWO) algorithm is employed in the feature selection process. AWO uses adaptive search mechanisms that enable it to adjust the feature selection process based on the characteristics of the dataset.

D. Feature Selection

The Adaptive Whale Optimization (AWO) algorithm is used for selecting features from MRIs. This optimization technique is inspired by the foraging behavior of whales and aims to enhance the efficiency of the feature selection process. By selecting the most relevant features using AWO from the MRI scans, the model's performance is improved by reducing noise and irrelevant information. Due to the shortcomings of whale optimization algorithms such as slow convergence speed, the insufficient ability of global optimization, and easily falling into local optimization: therefore, AWO is considered in this research. There are three stages included in the AWO approach which are as follows;

- Prey search
- Encircling prey
- Bubble-net feeding

1) Encircling prey

The Humpback whales detect the position of the prey and then encircle the prey. WOA's search agent is target prey which is also considered the best among other agents. During the iteration procedure, the position updates to the best searching agent about the location are achieved by utilizing humpback whales.

2) Bubble-net feeding

In the model, Spiral update posting, as well as shrinking encircling, are conducted sequentially for the humpback whale bubble-net attack technique.

3) Prey search

For the prey search, the shrinking encircling approach is used and also the coefficient vector $|\vec{A}| > 1$ is utilized as well to randomly choose the whale from the present population the location of the best search agent is modified. To increase the search space, a global search is performed where from the random whales the humpback whales are neglected.

E. Image Segmentation

Image segmentation is one of the important processes that involve dividing input images into segments for easy analysis. In this research, CNN and ResNeXt are used for image segmentation due to their high capability of segmenting and classifying images.

1) CNN

When contrasted to a deep Artificial Neural Network (ANN), CNNs have fewer parameters as well as a lesser training time. Therefore, CNNs have shown remarkable success in various computer vision tasks, including image segmentation, identification, as well as classification, due to their ability to capture complex patterns and spatial relationships. CNN segmentation as well as the classification system incorporates layers which include convolutional layers, pooling layers, fully connected layers, drop-out layers, etc. Fig. 2 shows the basic architecture of CNN.

In Fig. 2, the first layer's feature map is created by combining the input using six convolution kernels. Every convolution kernel is 5 × 5 in size, with a stride of 1. The following Eq. (5) is used to calculate the feature map size:

$$n_f = \frac{n_i + 2p - f}{s} \tag{5}$$

where,

n_f —feature map size

n_i —input data size

p —padding value

f —kernels size

s —stride value. The basic formula of a convolution operation is given in Eq. (6):

$$a^l = \delta(W^l a^{l-1} + b^l) \tag{6}$$

where,

a^l — lth convolution layer's output

W^l — lth convolution layer's convolution kernel

a^{l-1} — $l - 1$th convolution layer output

b^l — lth convolution layer's bias

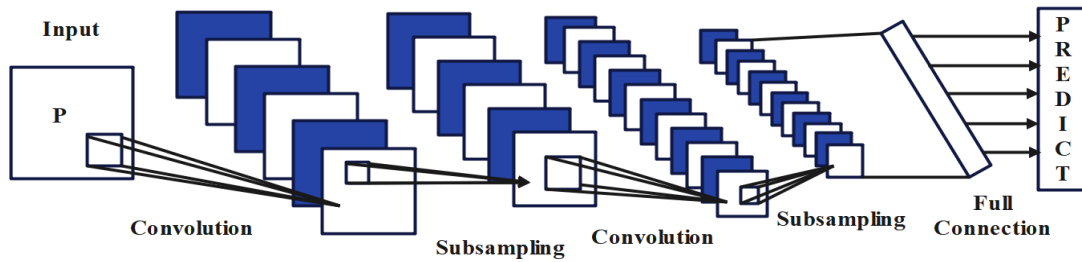δ — lth convolution layer's activation function.

Figure 2. Basic CNN architecture.

2) ResNeXt

ResNeXt is a framework that relies on the basic ResNet architecture whereas the ResNeXt model integrates the ResNet approach of recurring layers. Furthermore, ResNEXT was employed to deepen the model's capacity to capture intricate patterns and features within the data. The ResNEXT component utilized residual connections\blocks to facilitate the flow of information through the network, allowing for better gradient propagation and alleviating the vanishing gradient problem that affect conventional CNNs. This enhanced the model's ability to handle complex tumor structures and improve segmentation accuracy. The residual block not just increases network depth and also enhances system performance. The ResNeXt block with cardinality equals 32, with roughly a similar complexity is depicted in Fig. 3. Particularly, ResNeXt networks performed well in the ImageNet classification challenge. The residual block in ResNeXt performs the residual by combining the inputs with the residual block outcomes. The residual function is calculated as shown in Eq. (7):

$$y = F(x, W) + x \tag{3}$$

where,

x —residual block input

W —residual block weight
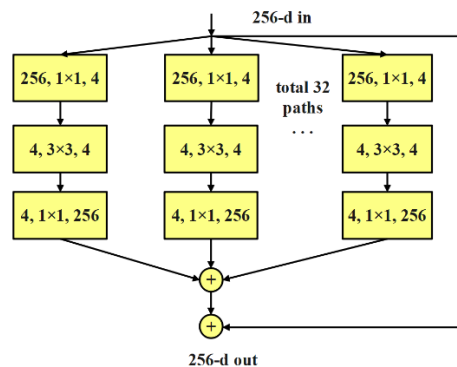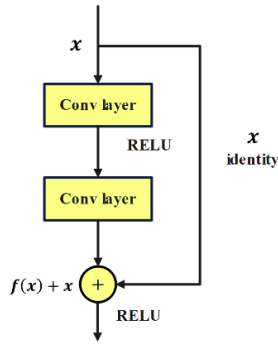
y —residual block output


Figure 3. ResNeXt block.

Figure 4. Residual block.

Here, Fig. 4 depicts the structure of the residual block. The ResNeXt network is made up of many residual blocks, each with a distinct convolution kernel size. The construction block is similar to the Inception network in that it allows several conversions such as 1×1 Conv, 3×3 Conv, 5×5 Conv, and MaxPooling. While the Inception model sequentially applies alterations, the ResNeXt model takes a different way by incorporating and merging them. The independent path value provides an additional level of cardinality to this model. It also provides conventional depth as well as height measurements.

Increasing cardinality allows the network to expand wider or deeper, which is extremely effective when the width as well as depth dimensions give lower outputs for typical models. The suggested ResNeXt building block comes in three types which are shown in Fig. 5. Experts stated that ResNeXt model is simple to train when compared with Inception network since it can be trained across numerous datasets. The segmented images are then sent into a classifier, which classifies brain tumors.
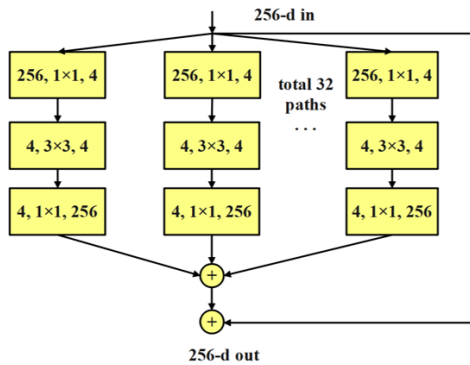
(a)
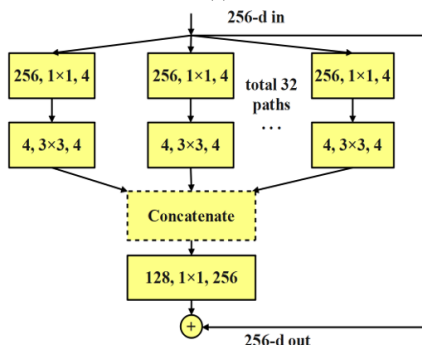
(b)
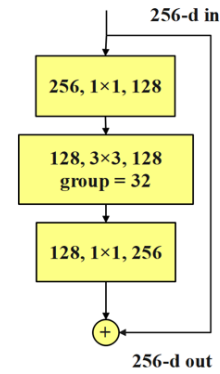
(c)

Figure 5. Equivalent building blocks of ResNeXt. (a) ResNeXt model. (b) A block equivalent to (a) implemented as early concatenation. (c) A block equivalent to (a, b), implemented as grouped convolutions).

F. Classification

The classification is performed to test the performance of the segmented feature set based on the classification method. Each classifier includes training and testing phases, where the dataset is also divided into training and validation datasets. In this research, a deep learning-based CNN and a transfer learning-based ResNeXt classifier is used for the effective classification of brain tumor. First, the segmented features are given as input to CNN-ResNeXt model then the classifier passes the images to their layers. Finally, the convolutional layers classify the image's features by scanning the input image with several filters.

IV. EXPERIMENTAL RESULTS

This section provides the results and analysis of the proposed CNN-ResNeXt model which is implemented and simulated using Python software whereas the computer is powered by the following parameters:

- RAM: 16GB
- Processor: INTEL i5
- Operating OS: Windows 10
- GPU: 6GB
- HDD: 1 TB

The common performance measures given in Table I are used to assess the performance of the proposed CNN-ResNeXt model.

TABLE I. PERFORMANCE MEASURES AND THEIR VALUES

Performance Measures	Values
Accuracy	$\frac{TP+TN}{TP+TN+FP+FN} \times 100$
Precision	$\frac{TP}{TP+FP} \times 100$
F-measure	$\frac{2PR}{P+R} \times \mathbf{100}$
Dice Similarity Coefficient (DSC)	$\frac{2TP}{FN+FP+2TP} \times 100$
Sensitivity	$\frac{TP}{TP+FN} \times 100$
Specificity	$\frac{TN}{TN+FP} \times 100$

A. *Performance Analysis*

The segmentation performance of the proposed CNN-ResNeXt model is analyzed and contrasted with conventional models: CNN, Visual Geometry Group (VGG-Net) and Residual Network (ResNet) in terms of sensitivity, and specificity, which are given in Table II. Where, the Tumor Core (TC), Whole Tumor (WT), and Enhanced Tumor (ET) are the tumor classes. Similarly, Table III represents the performance analysis of the CNN-ResNeXt model and other existing models in terms of DSC.

TABLE II. PERFORMANCE ANALYSIS OF PROPOSED MODEL WITH EXISTING MODELS

Methods	Performance Measures (%)					
	Sensitivity			Specificity		
	TC	ET	WT	TC	ET	WT
CNN	75	69	85	91	92	92
VGG-net	83	75	89	93	94	95
ResNet	90	85	91	95	94	97
CNN-ResNeXt	95	95	98	99.8	99.9	99.6

TABLE III. PERFORMANCE ANALYSIS OF PROPOSED CNN-RESNEXT MODEL WITH EXISTING MODELS IN TERMS OF DICE SIMILARITY COEFFICIENT (DSC)

Methods	DSC (%)		
	TC	ET	WT
CNN	80	70	85
VGG-net	89	81	90
ResNet	94	95	91
CNN-ResNeXt	97	98	94

Table II and Table III, show that the existing model CNN achieved the Sensitivity for TC, ET, and WT classes as 75%, 69%, and 85%, respectively, VGG-Net achieved the Sensitivity for TC, ET, and WT as 83%, 75%, and 89%, then finally ResNet achieved the Sensitivity for TC, ET, and WT as 93%, 94%, and 95%, respectively. CNN achieved the Specificity for TC, ET, and WT at 91%, 92%, and 92%, respectively, VGG achieved the Specificity for TC, ET, and WT at 93%, 94%, and 95%, then finally ResNet achieved the Specificity for TC, ET, and WT at 95%, 94%, and 97%, respectively. The DSC values achieved by CNN for TC, ET, and WT are 80, 70, and 85, respectively, DSC values achieved by VGG-net for TC, ET, and WT are 89%, 81%, and 90%, respectively. The DSC values achieved by ResNet for TC, ET, and WT are 94%, 95%, and 91%, respectively. Whereas the new proposed CNN-ResNeXt model achieved the Sensitivity for TC, ET, and WT as 95%, 95%, and 98%, respectively, Specificity for TC, ET, and WT as 99%, 99%, and 99%, respectively, and DSC for TC, ET, and WT as 97%, 98%, and 94%, respectively. From the analysis, the CNN-

ResNeXt model outperforms the other compared existing models. The graphical comparison of the obtained performance is illustrated in Figs. 6–8.
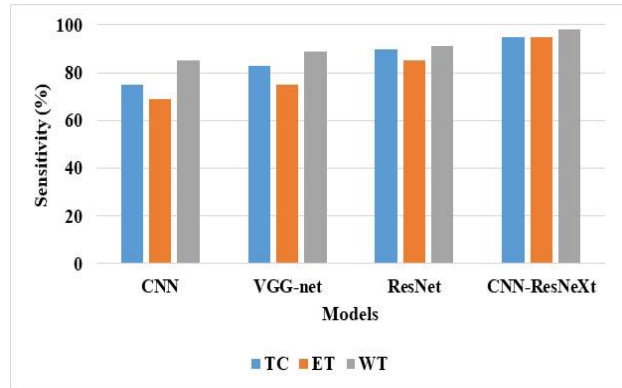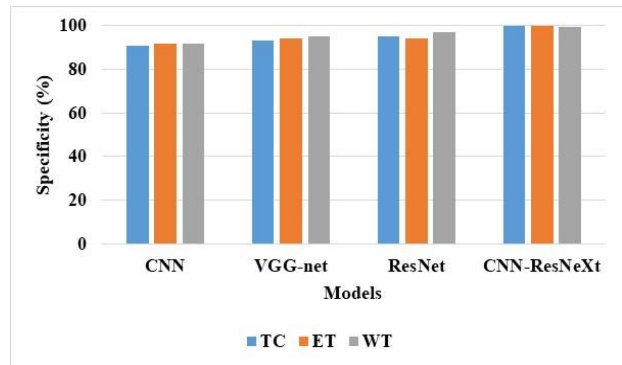

Figure 6. Analysis of Sensitivity.

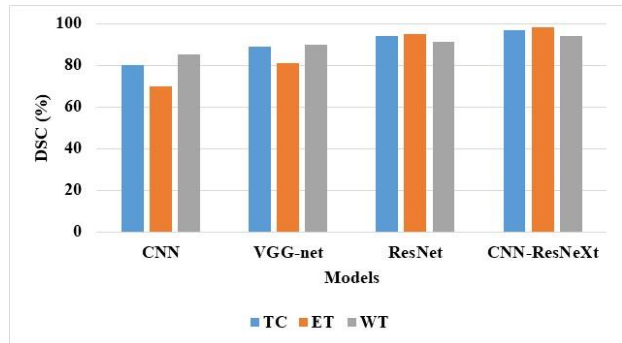Figure 7. Analysis of Specificity.

Figure 8. Analysis of DSC.

Similarly, the classification performance of the proposed CNN-ResNeXt model is analyzed as well as contrasted with conventional models which are given in Table IV.

TABLE IV. CLASSIFICATION PERFORMANCE OF PROPOSED CNN-RESNEXT IN TERMS OF ACCURACY, PRECISION AND F-MEASURE

Methods	Performance Measures (%)								
	Accuracy			Precision			F-measure		
	TC	ET	WT	TC	ET	WT	TC	ET	WT
CNN	85	77	82	80	69	84	90	91	94
VGG-net	92	88	88	87	78	90	94	94	96
ResNet	95	92	89	92	87	94	96	95	96
CNN-ResNeXt	99.2	98.7	98.9	98	98.3	97.9	98.6	99	98.2

From Table IV, the CNN achieved accuracies for classes TC, ET, and WT at 85%, 77%, and 82%, correspondingly. VGG-Net achieved accuracies for TC, ET, and WT at 92%, 88%, and 88%, correspondingly. ResNet achieved the accuracies for TC, ET, and WT at 95%, 92%, and 89%, correspondingly. Similarly, CNN achieved the precisions for TC, ET, and WT at 80%, 69%, and 84%, correspondingly. VGG-Net achieved the precisions for TC, ET, and WT at 87%, 78%, and 90%, correspondingly. Res-Net achieved the precisions for TC, ET, and WT at 92%, 87%, and 94%, correspondingly. Likewise, CNN achieved the F-measure for TC, ET, and WT at 90%, 98.7%, and 94%, correspondingly. VGG-Net achieved the F-measure for TC, ET, and WT at 94%, 94%, and 96%, correspondingly, and Res-Net achieved the F-measure for TC, ET, and WT at 96%, 95%, and 96%, correspondingly. Whereas the new proposed CNN-ResNeXt model achieved the accuracies for TC, ET, and WT at 99.2%, 98.7%, and 98.9%. The precisions for TC, ET, and WT were measured at 98%, 98.3%, and 97.9%, and the F-measures for TC, ET, and WT were measured at 98.6%, 99%, and 98.2%, correspondingly. From the analysis, the CNN-ResNeXt model outperforms the other compared existing models.

B. Comparative Analysis:

The overall comparison evaluation of the proposed CNN-ResNeXt model with the existing models such as Hybrid-DANet [18], Weighted Label Fusion learning Framework (WLFS) [20] and Residual Network (ResNet) [21] is given in Table V.

TABLE V. COMPARATIVE ANALYSIS OF PROPOSED CNN-RESNEXT MODEL WITH EXISTING MODELS IN TERMS OF SENSITIVITY AND SPECIFICITY

Methods	B RATS Dataset	Performance Measures (%)					
		Sensitivity			Specificity		
		TC	ET	WT	TC	ET	WT
HybridDANet [18]	2017	76.1	68.0	89.2	99.8	99.9	99.8
WLFS [20]	2015	88.7	88.12	89.32	99.4	99.2	99.6
	2017	87.7	86.9	88.6	98.8	98.7	99.1
	2019	88.6	89.2	90.05	99.4	99.3	99.7
ResNet [21]	2015	-	-	-	83	91	91
CNN-ResNeXt	2015	95	95	98	99.8	99.9	99.8
	2017	96	96.2	98.1	99.7	99.8	99.9
	2019	96.5	96	98.2	99.6	99.7	99.6

From Table V, the proposed CNN-ResNeXt model outperforms the other compared existing models in terms of Sensitivity and Specificity. While Table VI represents the comparative analysis in terms of DSC. The DSC values achieved by CNN-ResNext for TC, ET, and WT are 97%, 98%, and 94%, respectively for BraTs 2015 dataset. Correspondingly, The DSC values achieved by CNN-ResNext for TC, ET, and WT are 98%, 98.2%, and 95%, respectively for BraTs 2017 dataset. The DSC values achieved by CNN-ResNext for TC, ET, and WT are 97.5%, 97.9%, and 96%, respectively for BraTs 2019 dataset. From the analysis, the CNN-ResNeXt model outperforms the other compared existing models.

TABLE VI. COMPARATIVE ANALYSIS OF PROPOSED CNN-RESNEXT MODEL WITH EXISTING MODELS IN TERMS OF DSC

Methods	Dataset (BRATS)	DSC (%)		
		TC	ET	WT
Hybrid-DANet [18]	2017	76	68	89
WLFS [20]	2015	89.41	90.16	89.32
	2017	87.25	88.65	90.03
	2019	88.73	89.02	90.14
ResNet [21]	2015	93	96	86
MI-UNET [24]	2015	74.6	71.8	89.6
	2017	78.3	75.1	84
	2019	75.8	75.5	83.9
CNN-ResNeXt	2015	97	98	94
	2017	98	98.2	95
	2019	97.5	97.9	96

V. CONCLUSION

Accurate brain tumor segmentation plays a vital role in detecting tumors from patients or individuals who are suffering from a brain tumor. Firstly, the MRI images are collected from the publically available standard datasets named BRATS 2015, BRATS 2017 and BRATS 2019. Secondly, the batch normalization technique is used in the preprocessing stage to enhance the quality of the image. Then, the features are extracted from the enhanced images using the AlexNet model. After that, the optimal features are selected using the AWO feature selection approach. Then, the selected features are segmented and classified using the proposed CNN-ResNeXt model whereas the performance of the proposed CNN-ResNeXt model is contrasted with the conventional models which include CNN-SVM, U-Net and ResNet. The proposed CNN-ResNeXt model minimizes the number of hyperparameters needed by conventional network models. This is accomplished by the usage of "cardinality", an extra dimension on top of the width and depth of ResNet. While cardinality describes the size of the transformations set. Therefore, the researchers conducted experiments to illustrate the significance of an extra dimension in the network model which increases the classification accuracy. When compared to existing models the CNN-ResNeXt model achieves a greater sensitivity of 98%, specificity of 99.9%, and DSC of 98%. From the overall comparison analysis, the outcomes show that the proposed CNN-ResNeXt model outperforms the other conventional models in terms of DSC, Sensitivity, and Specificity. In the future, hyperparameters tuning will be performed in the classifier to achieve more accurate results.

CONFLICT OF INTEREST

The authors declare no conflict of interest.

AUTHOR CONTRIBUTIONS

Gayathri T. conducted the research, analyzed the data, and wrote the paper, collected and preprocessed the data. Sundeep Kumar K. analyzed and improved the proposed approach and reviewed the paper. All authors had approved the final version.

REFERENCES

[1] S. Tankala, G. Pavani, B. Biswal, G. Siddartha, G. Sahu, N. B. Subrahmanyam, and S. Aakash, "A novel depth search based light weight CAR network for the segmentation of brain tumor from MR images," *Neuroscience Informatics*, vol. 2, no. 4, 100105, December 2022.

[2] J. W. Sun, W. Chen, S. T. Peng, and B. Q. Liu, "DRRNet: Dense residual refine networks for automatic brain tumor segmentation," *Journal of Medical Systems*, vol. 43, pp. 1–9, 2019.

[3] P. Agrawal, N. Katal, and N. Hooda, "Segmentation and classification of brain tumor using 3D-UNet deep neural networks," *International Journal of Cognitive Computing in Engineering*, vol. 3, pp. 199–210, Jun. 2022.

[4] R. Ranjbarzadeh, A. B. Kasgari, S. J. Ghoushchi, S. Anari, M. Naseri, and M. Bendechache, "Brain tumor segmentation based on deep learning and an attention mechanism using MRI multi-modalities brain images," *Scientific Reports*, vol. 11, 10930, May 2021.

[5] N. Kesav and M. G. Jibukumar, "Efficient and low complex architecture for detection and classification of Brain Tumor using RCNN with Two Channel CNN," *Journal of King Saud University-Computer and Information Sciences*, vol. 34, no. 8B, pp. 6229–6242, Sep. 2022.

[6] J. Zhang, Z. Jiang, J. Dong, Y. Hou, and B. Liu, "Attention gate resU-Net for automatic MRI brain tumor segmentation," *IEEE Access*, vol. 8, pp. 58533–58545, Mar. 2020.

[7] T. Zhou, S. Canu, P. Vera, and S. Ruan, "Latent correlation representation learning for brain tumor segmentation with missing MRI modalities," *IEEE Transactions on Image Processing*, vol. 30, pp. 4263–4274, Apr. 2021.

[8] J. Sun, J. Li, and L. Liu, "Semantic segmentation of brain tumor with nested residual attention networks," *Multimedia Tools and Applications*, vol. 80, no. 26–27, pp. 34203–34220, Nov. 2021.

[9] M. Kolla, R. K. Mishra, S. Z. U. Huq, Y. Vijayalata, M. V. Gopalachari, and K. N. A. Siddiquee, "CNN-based brain tumor detection model using local binary pattern and multilayered SVM classifier," *Computational Intelligence and Neuroscience*, 9015778, Jun. 2022.

[10] P. Liu, Q. Dou, Q. Wang, and P. A. Heng, "An encoder-decoder neural network with 3D squeeze-and-excitation and deep supervision for brain tumor segmentation," *IEEE Access*, vol. 8, pp. 34029–34037, Feb. 2020.

[11] C. Yan, J. Ding, H. Zhang, K. Tong, B. Hua, and S. Shi, "SEResU-net for multimodal brain tumor segmentation," *IEEE Access*, vol. 10, pp. 117033–117044, Oct. 2022.

[12] Y. Ding, W. Zheng, J. Geng, Z. Qin, K. K. R. Choo, Z. Qin, and X. Hou, "MVFusFra: A multi-view dynamic fusion framework for multimodal brain tumor segmentation," *IEEE Journal of Biomedical and Health Informatics*, vol. 26, no. 4, pp. 1570–1581, Apr. 2022.

[13] Y. Liu, F. Mu, Y. Shi, and X. Chen, "Sf-net: A multi-task model for brain tumor segmentation in multimodal MRI via image fusion," *IEEE Signal Processing Letters*, vol. 29, pp. 1799–1803, Aug. 2022.

[14] M. A. Ottom, H. A. Rahman, and I. D. Dinov, "Znet: Deep learning approach for 2D MRI brain tumor segmentation," *IEEE Journal of Translational Engineering in Health and Medicine*, vol. 10, 1800508, May 2022.

[15] R. Pitchai, P. Supraja, A. H. Victoria, and M. Madhavi, "Brain tumor segmentation using deep learning and fuzzy K-means clustering for magnetic resonance images," *Neural Processing Letters*, vol. 53, no. 4, pp. 2519–2532, Aug. 2021.

[16] N. Micallef, D. Seychell, and C. J. Bajada, "Exploring the U-Net++ model for automatic brain tumor segmentation," *IEEE Access*, vol. 9, pp. 125523–125539, Sep. 2021.

[17] M. O. Khairandish, M. Sharma, V. Jain, J. M. Chatterjee, and N. Z. Jhanjhi, "A hybrid CNN-SVM threshold segmentation approach for tumor detection and classification of MRI brain images," *IRBM*, vol. 43, no. 4, pp. 290–299, Aug. 2022.

[18] N. Ilyas, Y. Song, A. Raja, and B. Lee, "Hybrid-DANet: An encoder-decoder based hybrid weights alignment with multi-dilated attention network for automatic brain tumor segmentation," *IEEE Access*, vol. 10, pp. 122658–122669, Nov. 2022.

[19] H. X. Hu, W. J. Mao, Z. Z. Lin, Q. Hu, and Y. Zhang, "Multimodal brain tumor segmentation based on an intelligent UNET-LSTM algorithm in smart hospitals," *ACM Transactions on Internet Technology*, vol. 21, no. 3, p. 74, Jun. 2021.

[20] L. H. Shehab, O. M. Fahmy, S. M. Gasser, and M. S. El-Mahallawy, "An efficient brain tumor image segmentation based on deep residual networks (ResNets)," *Journal of King Saud University-Engineering Sciences*, vol. 33, no. 6, pp. 404–412, Sep. 2021.

[21] S. Li, J. Liu, and Z. Song, "Brain tumor segmentation based on region of interest-aided localization and segmentation U-Net," *International Journal of Machine Learning and Cybernetics*, vol. 13, no. 9, pp. 2435–2445, Sep. 2022.

[22] A. R. Khan, S. Khan, M. Harouni, R. Abbasi, S. Iqbal, and Z. Mehmood, "Brain tumor segmentation using K-means clustering and deep learning with synthetic data augmentation for classification," *Microscopy Research and Technique*, vol. 84, no. 7, pp. 1389–1399, July 2021.

[23] S. Peng, Suting, W. Chen, J. Sun, and B. Liu, "Multi-scale 3d U-Nets: An approach to automatic segmentation of brain tumor," *International Journal of Imaging Systems and Technology*, vol. 30, no. 1, pp. 5–17, Mar. 2020.

[24] U. Latif, A. R. Shahid, B. Raza, S. Ziauddin, and M. A. Khan, "An end-to-end brain tumor segmentation system using multi-inception-UNET," *International Journal of Imaging Systems and Technology,* vol. 31, no. 4, 1803–1816, 2021.

[25] A. Işın, C. Direkoğlu, and M. Şah, "Review of MRI-based brain tumor image segmentation using deep learning methods," *Procedia Computer Science*, vol. 102, pp. 317–324, 2016.

[26] J. P. Liu *et al*., "IOUC-3DSFCNN: Segmentation of brain tumors via IOU constraint 3D symmetric full convolution network with multimodal auto-context," *Scientific Reports*, no. 1, 6256, 2010.

[27] C. Necip, A. Ozcan, and M. Kaya, "A hybrid densenet121-unet model for brain tumor segmentation from MR images," *Biomedical Signal Processing and Control*, vol. 76, 2022.